Journal of Mechanics Engineering and Automation 7 (2017) 50-57
doi: 10.17265/2159-5275/2017.01.007

Comparative Analysis between Conventional PI, Fuzzy Logic and Artificial Neural Network Based Speed Controllers of Induction Motor with Considering Core Loss and Stray Load Loss

Md. Rifat Hazari[1], Effat Jahan[1], Mohammad Abdul Mannan[2] and Junji Tamura[1]

1. Department of Electrical and Electronic Engineering, Kitami Institute of Technology, 165 Koen-cho, Kitami, Hokkaido 090-8507, Japan

2. Department of Electrical and Electronic Engineering, American International University-Bangladesh, Kemal Ataturk Avenue Banani, Dhaka 1213, Bangladesh

Abstract: Most of the controllers of IM (induction motor) for industrial applications have been designed based on PI controller without consideration of CL (core loss) and SLL (stray load loss). To get the precise performances of torque as well as rotor speed and flux, the above mentioned losses should be considered. Conventional PI controller has overshoot effect at the transient period of the speed response curve. On the other hand, fuzzy logic and ANN (artificial neural network) based controllers can minimize the overshoot effect at the transient period because they have the abilities to deal with the nonlinear systems. In this paper, a comparative analysis is done between PI, fuzzy logic and ANN based speed controllers to find the suitable control strategy for IM with consideration of CL and SLL. The simulation analysis is done by using Matlab/Simulink software. The simulation results show that the fuzzy logic based speed controller gives better responses than ANN and conventional PI based speed controllers in terms of rotor speed, electromagnetic torque and rotor flux of IM.

Key words: Core loss, stray load loss, PI controller, fuzzy logic controller, artificial neural network controller.

1. Introduction

Accuracy of the VC (vector control) or FOC (field oriented control) of IM drives mainly depends on the mathematical model because flux and torque decoupling control strategies have been developed based on dq-axes model of IM. Performance of the VC is also affected by variations of motor parameters and by the phenomena that are not modeled and therefore not accounted for in the model [1]. Among various losses, SLL has been often neglected in the mathematical modelling of IM. SLL is the portion of losses in a machine which cannot be accounted for by other losses such as friction and windage loss, stator I^2R loss, rotor I^2R loss, and core loss. It is also defined as additional losses representing a non-negligible term in the power balance of industrial induction machines [1, 2]. SLL inevitably appears in any ac machines and it has numerous sources. SLL in IM supplied from a power source is caused, in general, by higher flux density harmonics due to slotting effect, inter-bar rotor currents, and skewing.

Some literature reports the speed control of IM without considering CL and SLL [3, 4]. Some papers have presented a method of IM speed control with considering CL and SLL [1], where PI based speed controller is used to control the speed of IM [1]. But there can be seen some problems such as overshoot in the speed response curve of PI control based IM. This

Corresponding author: Md. Rifat Hazari, Ph.D. (ongoing), research fields: design and analysis of wind energy conversion system, analysis of power system dynamics, HVDC system, and analysis and control of rotating electrical machines.

is because gain parameters of PI controller are determined by trial and error method. In addition, the performance of PI controller can be decreased under uncertainties of motor parameters such as rotor resistance variation. The above-mentioned issue may be resolved by incorporating a FLC (fuzzy logic controller) or ANN since both have the ability to solve problems about uncertainties or imprecise situations.

In this paper, comparative analysis is presented between PI, fuzzy logic, and ANN based speed controllers of IM. The aim of this study is to find the best speed controller of IM.

2. State Space Model of IM

The dynamic state space model of IM in a synchronously rotating reference frame with considering CL and SLL is shown in Fig. 1 [1, 5-7]. The CL is represented by the resistance R_c and SLL is represented by resistance R_{st}.

The differential equations of IM are derived from Fig. 1 as:

$$\left.\begin{aligned} \boldsymbol{v}_S &= R_S\boldsymbol{i}_S + L_{sl}\frac{d\boldsymbol{i}_S}{dt} + L_m\frac{d\boldsymbol{i}_m}{dt} + j\omega_{se}L_{sl}\boldsymbol{i}_S + j\omega_{se}L_m\boldsymbol{i}_m \\ v_r &= R_r\boldsymbol{i}_r + L_{sl}\frac{d\boldsymbol{i}_r}{dt} + L_m\frac{d\boldsymbol{i}_m}{dt} + j\left(\omega_{se}-\omega_{re}\right)L_{sl}\boldsymbol{i}_r \\ &+ j\left(\omega_{se}-\omega_{re}\right)L_m\boldsymbol{i}_m \end{aligned}\right\} \quad (1)$$

For squirrel cage rotor type of IM, $v_r = 0$.

$$\left.\begin{aligned} \phi_S &= L_{sl}\boldsymbol{i}_S + L_m\boldsymbol{i}_m \\ \phi_r &= L_{sl}\boldsymbol{i}_r + L_m\boldsymbol{i}_m \end{aligned}\right\} \quad (2)$$

$$\left.\begin{aligned} R_c\boldsymbol{i}_c &= L_m\frac{d\boldsymbol{i}_m}{dt} + j\omega_{se}L_m\boldsymbol{i}_m \\ R_{st}\boldsymbol{i}_{st} &= L_{rl}\frac{d\boldsymbol{i}_{rl}}{dt} + j\left(\omega_{se}-\omega_{re}\right)L_{rl}\boldsymbol{i}_{rl} \end{aligned}\right\} \quad (3)$$

$$\left.\begin{aligned} \boldsymbol{i}_S + \boldsymbol{i}_r &= \boldsymbol{i}_m + \boldsymbol{i}_c \\ T_e &= P_n\left[i_{dr}\phi_{qr} + i_{qr}\phi_{dr}\right] \end{aligned}\right\} \quad (4)$$

$$\boldsymbol{i}_{st} = \boldsymbol{i}_r - \boldsymbol{i}_{rl} \quad (5)$$

$$\boldsymbol{i}_c = \boldsymbol{i}_S + \boldsymbol{i}_r - \boldsymbol{i}_m \quad (6)$$

$$\phi_m = L_m\boldsymbol{i}_m \quad (7)$$

$$\phi_S = L_{sl}\boldsymbol{i}_S + \phi_m = L_{sl}\boldsymbol{i}_S + L_m\boldsymbol{i}_m \quad (8)$$

$$\phi_r = L_{rl}\boldsymbol{i}_{rl} + \phi_m = L_{rl}\boldsymbol{i}_{rl} + L_m\boldsymbol{i}_m \quad (9)$$

where, $v_s = v_{sd} + jv_{sq}$, $i_s = i_{sd} + ji_{sq}$ and $\Phi_s = \Phi_{sd} + j\Phi_{sq}$ are stator voltage, current and flux, respectively; v_r is rotor voltage; $i_r = i_{rd} + ji_{rq}$ and $\Phi_r = \Phi_{rd} + j\Phi_{rq}$ are rotor current and flux, respectively; $i_m = i_{md} + ji_{mq}$, $i_c = i_{cd} + ji_{cq}$, $i_{rl} = i_{rld} + ji_{rlq}$ and $i_{st} = i_{std} + ji_{stq}$ are magnetizing current, core loss branch current, rotor leakage branch current and stray load loss branch current, respectively; ω_{se} and ω_{re} are synchronous angular velocity in electrical *rad/s* and rotor angular velocity in electrical

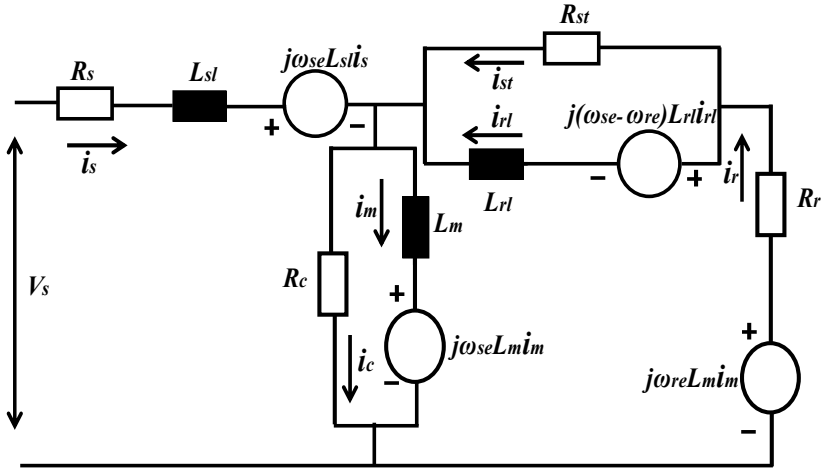

Fig. 1 Dynamic equivalent circuit of IM with considering CL and SLL.

rad/sec, respectively; $\omega_{rm} = \omega_{re}/P_n$ is rotor angular speed in mechanical *rad/sec*; P_n is the number of poles; T_e and T_L are electromagnetic torque and load torque, respectively; R_s, R_r, R_c and R_{st} are stator, rotor, core loss and stray load loss resistances, respectively; L_{sl}, L_{rl}, and L_m are stator leakage, rotor leakage, and mutual inductances, respectively; $L_s = L_{sl} + L_m$ and $L_r = L_{rl} + L_m$ are stator and rotor self-inductances, respectively; B_m and J_m are friction coefficient and moment of inertia, respectively.

Using Eqs. (1)-(9), the state equations are:

$$\frac{d\phi_r}{dt} = R_r c_1 \boldsymbol{i}_S + R_r c_2 \boldsymbol{i}_m - R_r c_2 \phi_r - j\omega_r R_r c_4 \boldsymbol{i}_m - j\omega_{sl}\phi_r \quad (10)$$

$$\frac{d\boldsymbol{i}_m}{dt} = c_5 \boldsymbol{i}_S - c_6 \boldsymbol{i}_m + c_7 \phi_r - j\omega_{se}\boldsymbol{i}_m + jc_8\omega_{re}\boldsymbol{i}_m \quad (11)$$

$$\frac{d\boldsymbol{i}_S}{dt} = -c_9 \boldsymbol{i}_S + c_{10}\boldsymbol{i}_m - c_{11}\phi_r - j\omega_{se}\boldsymbol{i}_S - jc_{12}\omega_{re}\boldsymbol{i}_m + d_1 \boldsymbol{v}_S \quad (12)$$

$$\frac{d\omega_r}{dt} = -c_{15}\omega_{re} + c_{16}(T_e - T_L) \quad (13)$$

where

$$c_1 = \frac{R_c}{R_{rsc}}; c_2 = \frac{R_{st}L_m - R_c L_{rl}}{R_{rsc}L_{rl}}; c_4 = \frac{L_m}{R_{rsc}}; c_5 = \frac{1-c_1}{T_c}; T_c = \frac{R_c}{L_m}$$

$$c_6 = \frac{1+c_2}{T_c}; c_7 = \frac{c_4}{T_c}; c_8 = \frac{c_4}{T_c}; c_9 = \frac{R_s + L_m c_5}{L_{sl}}; c_{10} = \frac{L_m c_4}{L_{st}};$$

$$c_{11} = \frac{L_m c_7}{L_{sl}}; c_{12} = \frac{L_m c_s}{L_{sl}}; c_{15} = \frac{D}{J}; c_{16} = \frac{P_n}{J}; d_1 = \frac{1}{L_{sl}}$$

3. Control Strategy of IM

The overall block diagram of the system composed of IM and controller is shown in Fig. 2, in which reference rotor flux (Φ_r^*) and reference rotor speed (ω_r^*) are controller inputs. In addition, d-axis current (I_d), q-axis current (I_q), stator d-axis voltage (V_{sd}), stator q-axis voltage (V_{sq}), rotor flux (Φ_r) and rotor speed (ω_r) are taken as feedback signal from IM.

The controller sends the reference stator d-axis voltage (V_{sd}^*), stator q-axis voltage (V_{sq}^*) and slip frequency (ω_{se}^*) to the IM for achieving desired responses of the IM. The detail about some possible advanced controllers of IM are discussed in the following subsections.

3.1 ANN Based Speed Controller

Fig. 3 shows the block diagram of the control system. The control system consists of three PI controllers (PI d-axis current controller, PI q-axis current controller and PI flux controller) and ANN based speed controller. The purpose of using the ANN based speed controller is to minimize the overshoot in the transient period. For the ANN based speed controller, error of speed and change in error of speed are taken as inputs and the output is multiplied with a scaling factor to obtain the original q-axis stator current (I_{sqt}).

ANNs are nonlinear data driven self-adaptive method as opposed to traditional methods. They can be a powerful tool for modeling the system of which underlying data relationship is unknown. ANNs can train themselves according to corrected patterns between input data sets and corresponding target data values. After training ANNs can be used to predict the outcome of new independent input data [8].

An ANN contains neurons and connection lines. A two-layer neural network is shown in Fig. 4, where layer 1 is called the hidden layer and layer 2 is called the output layer [9]. The internal structure of artificial neuron is depicted in Fig. 5. It contains of net weight (product operator), net bias (constant), net sum (add operator), and a transfer function.

The LM (levenberg-marquardt) back-propagation training algorithm is used in this study that updates

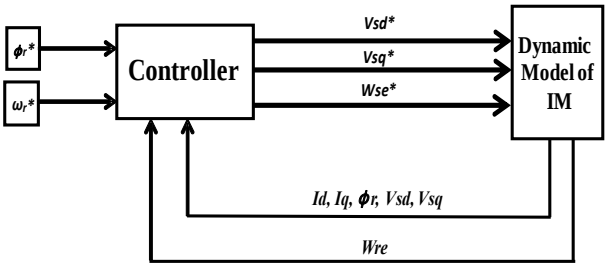

Fig. 2 Block diagram of IM along with its control system.

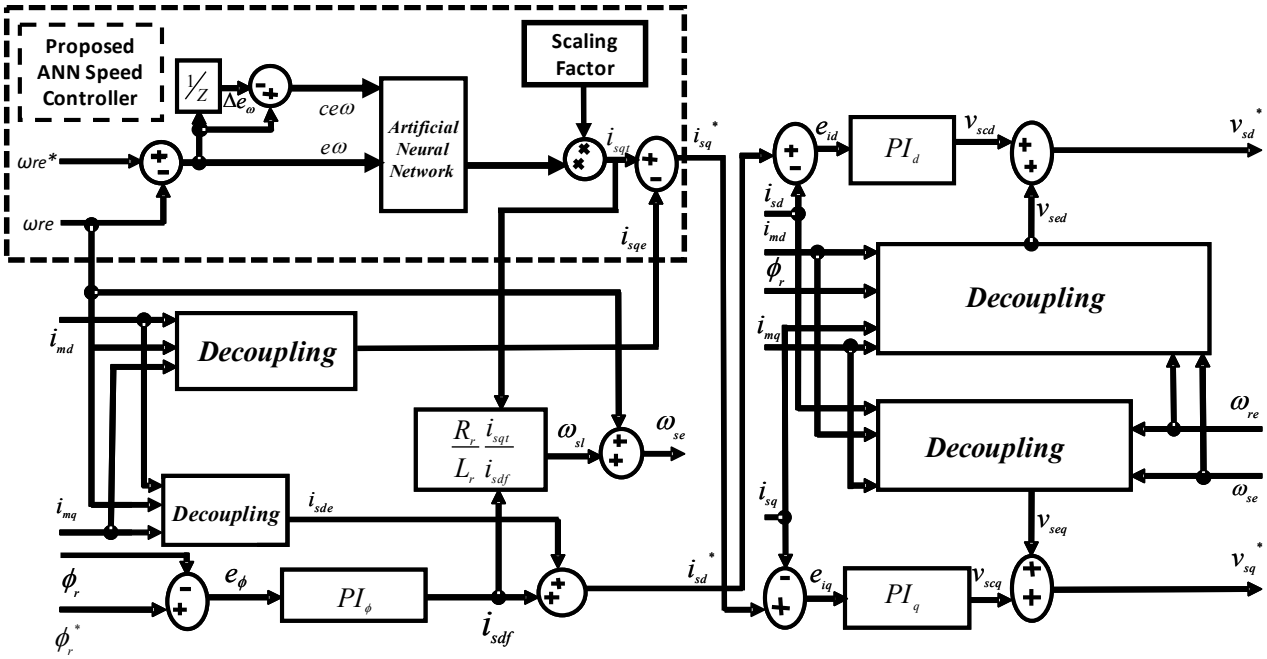

Fig. 3 Control system of IM with ANN based speed controller.

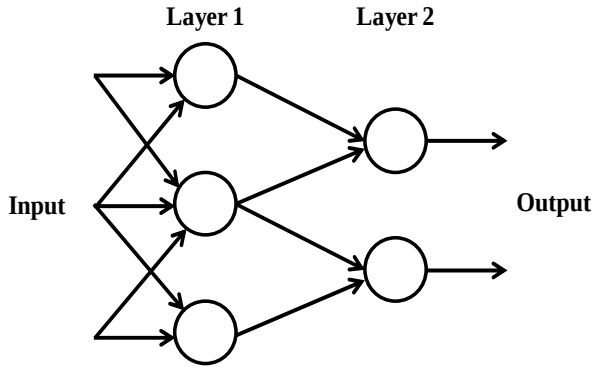

Fig. 4 Structures of ANN.

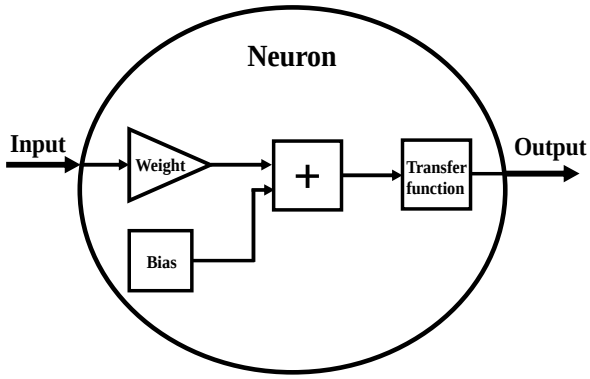

Fig. 5 Internal structure of artificial neuron.

weight and bias values according to LM optimization. The back-propagation training technique adjusts the weight and bias in all connecting links, so that the difference between the actual output and target output is minimized for all given training patterns. Normally, two hidden layers are sufficient to train a nonlinear pattern. Here, a Tan-Sigmoidal function is used in hidden layer and linear transfer function is used at output layer. Target values are obtained from PI speed controller. The parameters of ANN used in this study is depicted in Table 1.

3.2 FLC Based Speed Controller

Fuzzy Logic is an advanced technology that augments the conventional system design with engineering expertise. It is a linguistic based controller that tries to compete with the way of human thinking in solving a particular problem by means of rule interferences. It has the capabilities to deal with imprecise or noisy data.

Table 1 Parameters of ANN.

Number of input neurons	2
Number of output neurons	1
Number of hidden layer	2
Number of neurons in the hidden layers	10
Transfer function used at hidden layer	Transig
Transfer function used at output layer	Purelin

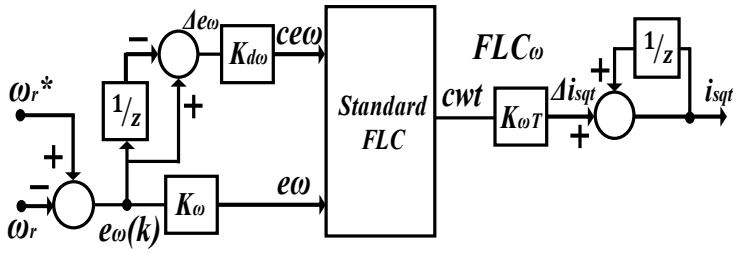

Fig. 6 FLC based speed controller. (Note: ω_r*= reference speed; ω_r= actual speed)

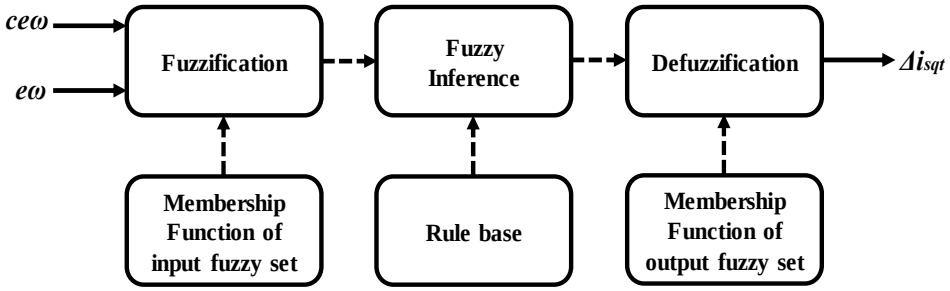

Fig. 7 General structure of FLC.

Fig. 6 shows the block diagram of the FLC. This FLC is obtained by replacing the ANN controller in Fig. 3 with fuzzy logic based speed controller.

The general structure of FLC is shown in Fig. 7. The FLC is composed of fuzzification, membership function, rule base, fuzzy inference and defuzzification.

The fuzzification includes the procedure of converting crisp values into grades of membership for linguistic terms of fuzzy sets. The membership function is used to associate a grade to each linguistic term. For fuzzification, the triangular membership functions with overlap are used for the input and output fuzzy sets as shown in Fig. 8, in which linguistic variables are represented as NB (negative big), NM (negative medium), NS (negative small), ZO (zero), PS (positive small), PM (positive medium), and PB (positive big).

The grade of input membership functions can be obtained as follows [10]:

$$\mu(x) = [w - 2(x - m)] / 2 \qquad (14)$$

where, $\mu(x)$ is the value of grade of membership, w is the width, m is the coordinate of the point at which the grade of membership is 1, and x is the value of input variable.

The rules of fuzzy mapping of the input variables to the output are represented as the following form:

IF <eω is PB> and <ceω is NS> THEN <cwt is PS>

IF <eω is NM> and <ceω is NS> THEN <cwt is NM>

The entire rule base is given in Table 2. There are total 49 rules in the table.

According to the rule base in the table, the inference engine provides fuzzy value of *cwt* and then crisp numerical value of Δi_{sqt} can be obtained by using defuzzification procedure. Different inference engines can be used to produce the fuzzy set values for the output fuzzy variable.

In this study, mamdani type fuzzy inference is used. The center of gravity method is used for defuzzification

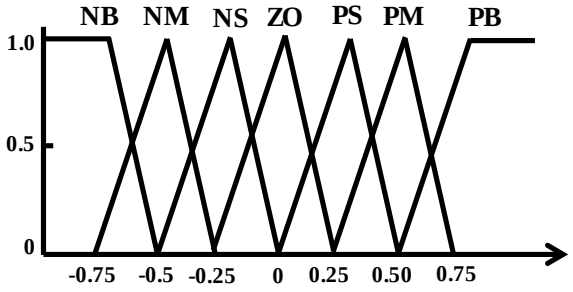

Fig. 8 Membership functions for inputs and output.

Table 2 Fuzzy rules.

cwt		*ceω*						
		NB	*NM*	*NS*	*ZO*	*PS*	*PM*	*PB*
	NB	NB	NB	NM	NM	NS	NS	ZO
	NM	NB	NM	NM	NS	NS	ZO	PS
	NS	NM	NM	NS	NS	ZO	PS	PS
eω	*ZO*	NM	NS	NS	ZO	PS	PS	PM
	PS	NS	NS	ZO	PS	PS	PM	PM
	PM	NS	ZO	PS	PS	PM	PM	PB
	PB	ZO	PS	PS	PM	PM	PB	PB

to obtain *cwt*. The normalized output function is given as Ref. [10],

$$i_{sqt} = \frac{\sum_{i=1}^{N} \mu_i(c\omega t) C_i}{\sum_{i=1}^{N} \mu_i(c\omega t)} \quad (15)$$

where, N is the total number of rules, $\mu_i(cwt)$ is the membership grade for i^{th} rule and C_i is the coordinate corresponding to the maximum value of the respective consequent membership function.

4. Simulation Results

The design of each speed controller of IM has been performed by using the state space equations and the entire system of Fig. 2 has been developed on the laboratory simulator Matlab/Simulink. The core motive behind the design of the advanced controllers is to trail the reference inputs and also to overcome the overshooting phenomena appeared in the conventional PI based speed controller.

The sampling time is taken as 200 μs. Specifications and parameters of IM are depicted in Tables 3 and 4.

Three cases are considered in this simulation study.

Case 1: Using four conventional PI controllers (PI speed controller, PI flux controller, PI d-axis current controller and PI q-axis current controller).

Case 2: Using one ANN speed controller and three conventional PI Controllers (PI flux controller, PI d-axis current controller and PI q-axis current controller).

Case 3: Using one FLC speed controller and three conventional PI Controllers (PI flux controller, PI d-axis current controller and PI q-axis current controller).

Table 3 Specifications of IM.

Rated voltage (V)	460
Rated power (hp)	7.5
Rated speed (rpm)	1,436
Rated frequency (Hz)	50
Number of poles (P_n)	4
DC voltage (V)	400

Table 4 Parameters of IM.

Stator resistance, R_s (Ω)	0.638
Rotor resistance, R_r (Ω)	0.6395
Core loss resistance, R_c (Ω)	621.12
Stray load loss resistance, R_{st} (Ω)	2.19
Stator self-inductance,L_s(mH)	75.4
Rotor self-inductance,L_r (mH)	75.0

The rotor speed response of IM under the variation in reference speed is shown in Fig. 9 for all three cases. It is seen that in cases 2 and 3 there are no overshoot in the rotor speed but the overshoot is seen in case 1. In addition, the rotor speed responses in both case 2 (ANN based speed controller) and case 3 (FLC based speed controller) are identical.

The electromagnetic torque variations in the transient period are much lower in case 3 than cases 1 and 2 as depicted in Fig. 10.

Finally, the rotor flux response of IM is illustrated in Fig. 11. The variation of rotor flux in the transient period is lower in case 3 than cases 1 and 2.

So, from the above discussions it can be concluded that in terms of rotor speed, electromagnetic torque and rotor flux response, the FLC based speed controller gives better performances than ANN and conventional PI based speed controllers.

5. Conclusions

In this paper, a comparative analysis is presented between conventional PI, ANN and FLC based speed controllers. The transient performances of IM controlled by each controller are investigated and compared. The simulation results show that the FLC based speed controller gives appreciable performance in terms of rotor speed, electromagnetic torque and rotor flux than the conventional PI and ANN based speed controllers.

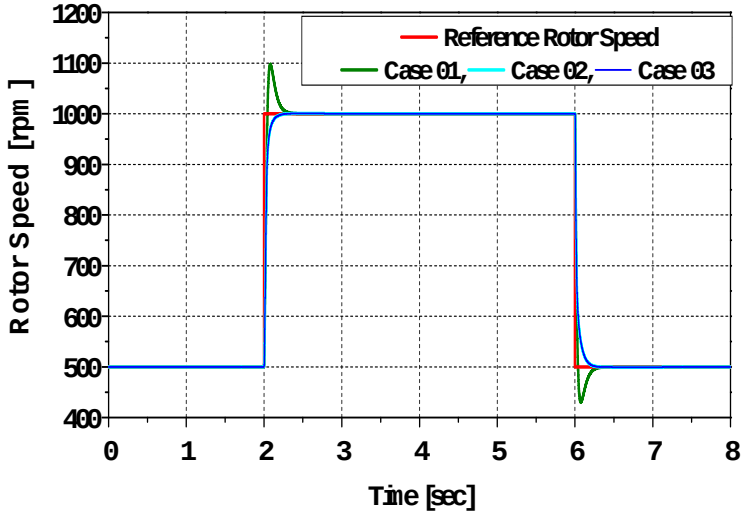

Fig. 9 Rotor speed response of IM under variation in reference speed.

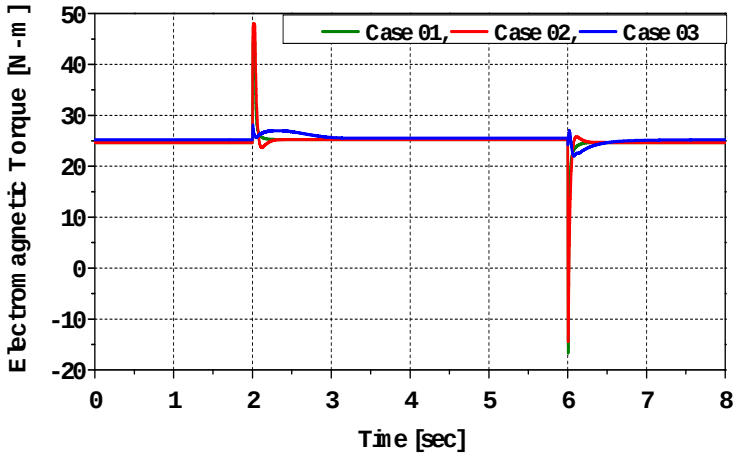

Fig. 10 Electromagnetic torque response of IM under variation in reference speed.

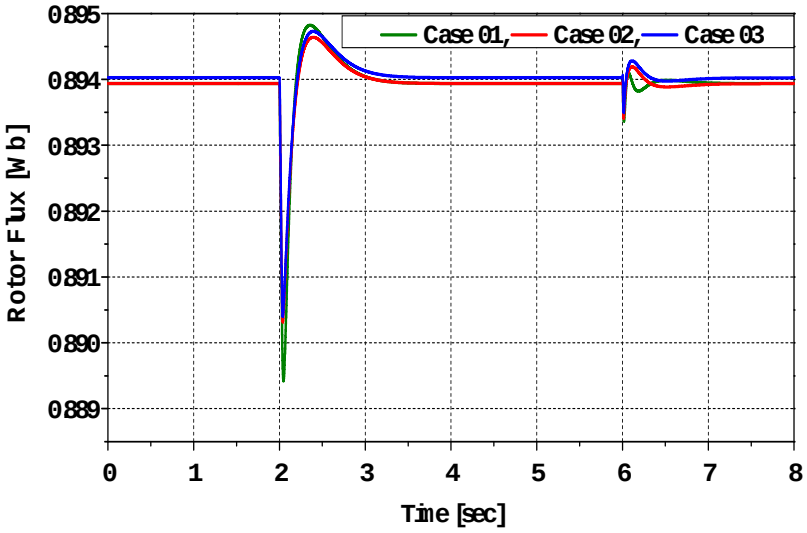

Fig. 11 Rotor flux response of IM under variation in reference speed.

Acknowledgements

The authors thank Dr. Rion Takahashi and Dr. Atsushi Umemura in Kitami Institute of Technology for their valuable comments and encouragement.

This study was supported by the Grant-in-Aid for Scientific Research (B) from The Ministry of Education, Science, Sports and Culture of Japan.

References

[1] Dhar, R. K., Haque, M. E., Taia, M. A., Sikdar, M. R., and Mannan, M. A. 2014. "Design and Simulation of Speed Control of an Induction Motor Taking Core Loss and Stray Load Losses into Account." Presented at the 2nd International Conference on Advances in Electrical Engineering, Dhaka, Bangladesh.

[2] Lamine, A. 2007. "Modelling and Detuning Assessment due to Stray Load Losses in Vector Controlled Induction Machines." Presented at the Industrial Electronics Society, IECON 33rd Annual Conference of the IEEE, Taipei, Taiwan.

[3] Orlowska-Kowalska, T., and Dybkowski, M. 2010. "Stator-Current-Based MRAS Estimator for a Wide Range Speed-Sensor Less Induction-Motor." *IEEE Trans. on Industry Electronics* 57 (4): 1296-308.

[4] Najafabadi, T. A., Salmasi, F. R., and Jabehdar-Maralani, P. 2011. "Detection and Isolation of Speed, DC-link Voltage, and Current-Sensor Faults Based on an Adaptive Observer in Induction-Motor." *IEEE Trans. on Industry Electronics* 58 (5): 1662-72.

[5] Levi, E., Lamine, A., and Cavagnino, A. 2006. "Impact of Stray Load Losses on Vector Control Accuracy in Current-fed Induction Motor Drives." *IEEE Trans. on Energy Conversion* 21 (2): 442-50.

[6] Levi, E., Lamine, A., and Cavagnino, A. 2005. "Detuned Operation of Vector Controlled Induction Machines due to Stray Load Losses." In *Proceedings of the Industry Applications Conference*, 500-7.

[7] Hazari, M. R., Mannan, M. A., Murata, T., and Tamura, J. 2014. "Design and Simulation of Discrete Time Optimal Speed Control for an Induction Motor Taking Core Loss and Stray Load Losses into Account." *Journal of Power Electronics and Power Systems, STM Journals* 4 (3): 46-56.

[8] Gorobetz, M., and Levchenkov, A. 2008. "Modeling of Artificial Neural Network Controller for Electric Drive in Virtual Laboratory." In *Proceedings of 7th International Conference Engineering for Rural Development,* 198-203.

[9] Chan, T., and Shi, K. 2011. *Applied Intelligent Control of Induction Motor Drives*. John Wiley & Sons (Asia) Pte Ltd.

[10] Driankov, D., Hellendoorn, H., and Reinfrank, M. 1993. *An Introduction to Fuzzy Control*. Berlin, Germany: Springer-Verlag.

[11] Hazari, M. R., Jahan, E., Mannan, M. A., and Tamura, J. 2015. "Design and Simulation of Fuzzy Logic Based Speed Control for an SVPWM Inverter-fed Induction Motor Considering Core Loss and Stray Load Losses." In *Proc. of IEEE International WIE Conference on Electrical and Computer Engineering*, 5-9.

[12] Vas, P. 1990. *Vector Control of AC Machines*. Oxford: Clarendon Press.

[13] Tewari, A. 2002. "Modern Control Design with Matlab and Simulink." *International Journal of Engineering Education* 21 (5): 896-905.

[14] Wlas, M., Krzemin´ski, Z., Guzin´ski, J., Abu-Rub, H., and Toliyat, H. A. 2005. "Artificial Neural Network Based Sensor Less Nonlinear Control of Induction Motors." *IEEE Trans. on Energy Conversion* 20 (3): 520-8.

[15] Bose, B. K. 2001. *Modern Power Electronics and AC Drives*. Prentice Hall.

[16] Chan, T., and Shi, K. 2011. *Applied Intelligent Control of Induction Motor Drives*. John Wiley & Sons (Asia) Ltd.